

Rotationally Resolved Electronic Spectra of the $\tilde{B}-\tilde{X}$ Transition in Multiple Conformers of 1-Butoxy and 1-Pentoxo Radicals

Sandhya Gopalakrishnan, Lily Zu, and Terry A. Miller*

Laser Spectroscopy Facility, Department of Chemistry, The Ohio State University,
120 West 18th Avenue, Columbus, Ohio 43210

Received: January 7, 2003; In Final Form: April 24, 2003

We report the rotational analyses of six bands of the $\tilde{B}-\tilde{X}$ electronic transition of jet-cooled 1-butoxy radical and 11 bands of the corresponding transition in 1-pentoxo radical. From these spectra, we have obtained experimental values for the rotational and spin-rotational constants in the \tilde{X} state and the rotational constants, vibrational frequencies, and band origins in the \tilde{B} state. By comparing the rotational and spin-rotational constants from these analyses with corresponding values from quantum chemistry computations, we assign the observed spectra to the electronic origins and excited vibrational levels of the \tilde{B} state of three distinct conformers of 1-butoxy and five distinct conformers of 1-pentoxo. These assigned bands can be used as unambiguous diagnostics of the radical species, its structural isomer, and its conformation. These data can be used to identify, and to some extent rationalize, distinctively different conformer stabilities in the \tilde{X} and \tilde{B} states and conformer-dependent dynamical behavior.

1. Introduction

Free radicals are key components in the oxidation of hydrocarbons both in combustion and in our atmosphere. Among the simplest oxygen-containing organic radicals are the alkoxy (RO) species. The spectroscopy of the smallest alkoxy radicals is well studied, detailed spectral analyses having been reported for $\text{CH}_3\text{O}^{1-6}$ and $\text{C}_2\text{H}_5\text{O}^{7-10}$ and less detailed work on isopropoxy, 2- $\text{C}_3\text{H}_7\text{O}^{11-13}$. More recently, the laser-induced fluorescence (LIF) spectra of 2- and *t*-butoxy and 3- and *t*-pentoxo have been reported.^{14,15} Soon thereafter, we reported¹⁶ the jet-cooled, moderate-resolution $\tilde{B}-\tilde{X}$ LIF spectra of all of the primary and secondary radicals from propoxy to decoxy, that is, 1- $\text{C}_n\text{H}_{2n+1}\text{O}$ and 2- $\text{C}_n\text{H}_{2n+1}\text{O}$, $n = 3-10$.

In a recent paper, we reported the analyses of the rotational structure¹⁷ in the high-resolution spectra of a number of bands of 1-propoxy. Using the rotational analysis to “bar code” the observed bands, we were able to assign them to two different conformers of 1-propoxy. In this paper, the spectroscopy of the next two alkoxy radicals in the homologous series, namely, 1-butoxy and 1-pentoxo, will be discussed along similar lines. The survey spectra of these radicals are shown in panels a and b of Figure 1, respectively. The bands labeled A through F in Figure 1a and *a* through K in Figure 1b were studied under high resolution to resolve their rotational structure.

Rotationally resolved spectra of bands of 1-butoxy are labeled A–F in Figure 2. As this figure shows, three unique sets of bands can immediately be distinguished upon the basis of rotational structure: band A in one group, bands B, D, and F in the second, and bands C and E in the third. We reported a similar observation in the case of 1-propoxy.¹⁷ In that work, the difference in rotational structure between different groups of vibronic bands was confirmed to be due to the two different conformers of the 1-propoxy radical by means of detailed rotational analysis. It is likely that the three sets of bands of 1-butoxy shown in Figure 2 are also ascribable to different conformers of this radical.

The number of conformations available for molecules belonging to a homologous series increases dramatically as the number

of skeletal atoms (carbon atoms in the case of the alkoxy radicals) increases. Thus, we expect the spectroscopy of 1-butoxy to be more complicated than that of 1-propoxy, as indeed Figure 2 demonstrates. The lowest frequency band in each group is considered to be the apparent origin of the particular conformer. The other higher frequency bands in each group are most likely vibrationally excited bands of the particular conformer.

As expected, the situation gets even more complicated in the case of 1-pentoxo. Figures 3 and 4 show the rotationally resolved spectra of bands *a* through K of 1-pentoxo. Six groups of bands can be distinguished upon the basis of vastly different rotational structure: bands A and G belong to one group, bands C, F, J, and K belong to the second, bands B and I belong to the third, band *a* belongs to the fourth, bands E and H belong to the fifth, and band D belongs to the sixth. Thus the high-resolution spectra of 1-pentoxo shows the presence of at least six different conformers.

In the remainder of this paper, we will detail the rotational analysis of the spectra shown in Figures 2, 3, and 4. These analyses will result in a detailed set of molecular constants (rotational and spin-rotational) for the states and species involved. These data serve to confirm the presence of multiple conformers of the radicals and the corresponding vibronic assignment of these bands using the “rotational bar-coding” technique. Once the precise identity of each band is established, it can be a diagnostic of the species. Using this approach, we comment upon the conformer selectivity and relative stability and speculate on the decay dynamics of different quantum levels of the \tilde{B} state of 1-butoxy and 1-pentoxo.

2. Experimental Section

The alkoxy radicals were generated in a supersonic free-jet expansion by UV laser photolysis (XeF) of the corresponding alkyl nitrites at the base of a 0.5 mm circular nozzle. The alkyl nitrites were synthesized according to well-known procedures.¹⁸ A few torr of the alkyl nitrite vapor was forced into the jet flow by passing helium at 200 psi over the liquid contained in a steel bomb maintained at a suitable temperature depending upon the vapor pressure.

The rotationally resolved spectra of the alkoxy radicals were obtained using our high-resolution apparatus. This has been

* Corresponding author.

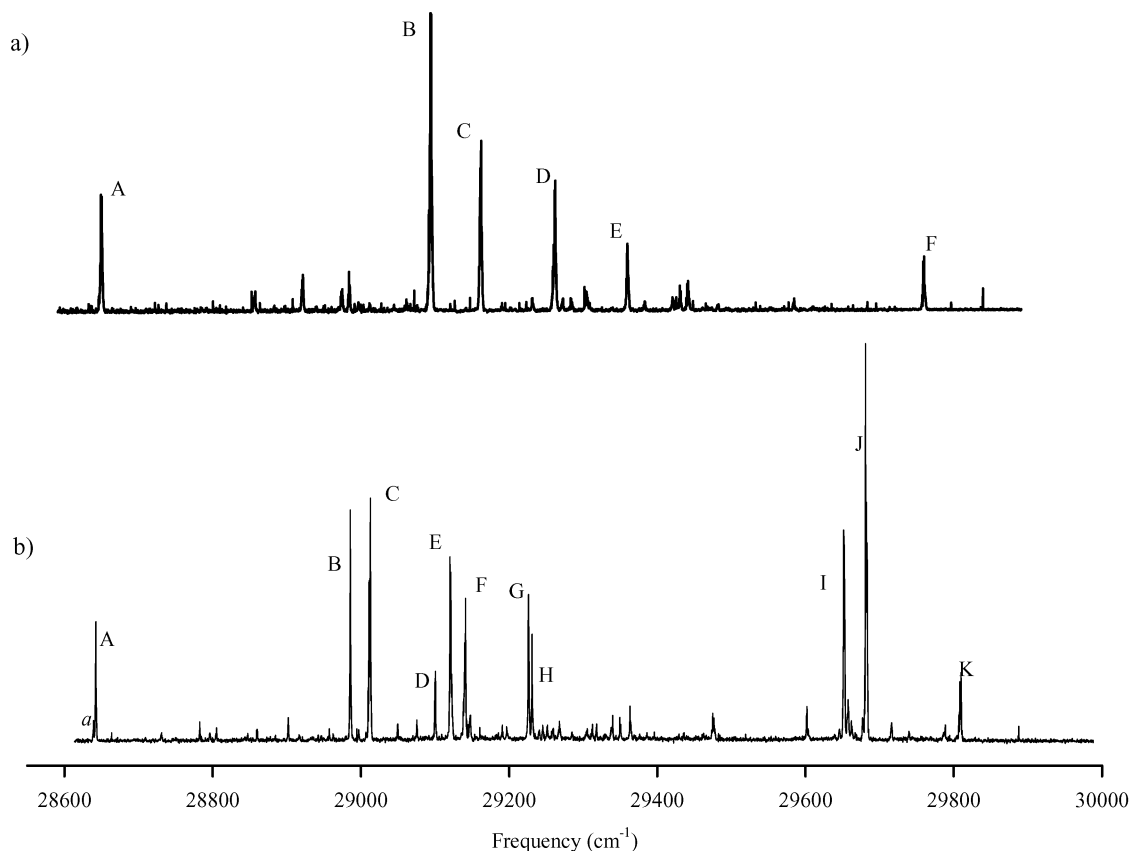


Figure 1. Survey LIF spectra of (a) 1-butoxy and (b) 1-pentoxy. Labeled bands have been rotationally analyzed.

described in detail elsewhere.^{19–21} Only a brief description will be provided here. A CW ring dye laser (Coherent 899-29 Autoscan) pumped by an Ar⁺ laser (Coherent Innova Sabre) was pulse-amplified and frequency-doubled using a KDP crystal to generate the UV radiation required to pump the $\tilde{B}-\tilde{X}$ transition of the alkoxy radicals. The pulse amplifier (Lambda Physik, FL 2003 model) was pumped by an excimer laser (XeCl, Lambda Physik, MSC 103 model) with resulting line width of ~ 100 MHz in the fundamental (200 MHz in the UV). This radiation was directed into a vacuum chamber ~ 16 mm downstream to pump the transition. The resulting fluorescence is collected perpendicular to the probe laser beam with a 2.5 cm f/1 lens. This is then focused with an f/3 lens through an adjustable slit onto a photomultiplier tube. The slit can be adjusted to allow only the central portion of the fluorescence from the jet to be detected by the photomultiplier tube (PMT) to reduce the Doppler width of the signal from off-axis velocity components in the jet expansion. This signal is then preamplified and sent to a boxcar averager (Stanford Research, SR250 boxcar) for integration and then through an amplifier. This amplified signal was then sent to the Coherent Autoscan for signal averaging and recording.

3. Theory

The basic theory underlying the analysis of the rotational structure of the bands was developed in ref 17 and will be only briefly described here. The primary alkoxy radicals (except methoxy) are asymmetric tops and thus the rotational structure of their high-resolution electronic spectra may be modeled by an asymmetric top Hamiltonian (\mathcal{H}_{Rot}). Centrifugal distortion terms may be neglected because of the very low rotational temperature achieved in the jet. Typically, rotational levels with $J > 5$ are not populated. However, it is necessary to add a spin-

rotation Hamiltonian (\mathcal{H}_{SR}) to model the fine structure of the bands. Thus the total effective Hamiltonian may be written

$$\mathcal{H} = \mathcal{H}_{\text{Rot}} + \mathcal{H}_{\text{SR}} \quad (1)$$

Denoting the rotational angular momentum by \mathbf{N} and the spin angular momentum by \mathbf{S} , we may expand^{22,23} both \mathcal{H}_{Rot} and \mathcal{H}_{SR} :

$$\mathcal{H}_{\text{Rot}} = AN_a^2 + BN_b^2 + CN_c^2 \quad (2)$$

$$\mathcal{H}_{\text{SR}} = \frac{1}{2} \sum_{\alpha, \beta} \epsilon_{\alpha\beta} (N_\alpha S_\beta + S_\beta N_\alpha) \quad (3)$$

Here, A , B , and C are the conventional rotational constants, and $\epsilon_{\alpha\beta}$ are the components of the spin-rotation tensor in the inertial axis system (a , b , c).

The matrix elements of \mathcal{H} in a Hund's case (b) like symmetric top basis set $|JNKSM_J\rangle$ where \mathbf{J} is the total angular momentum have been described previously¹⁷ and will not be discussed here. Likewise, the calculation of the eigenvalues of \mathcal{H} and the rotational intensities of transitions between the \tilde{B} and \tilde{X} states have been previously discussed.¹⁷ However it is important to bear in mind the number of spectroscopic parameters that need to be fit to the high-resolution spectra. The six rotational constants, namely, A'' , B'' , and C'' in the ground state and A' , B' , and C' in the excited \tilde{B} state, need to be fit to the spectra. Equation 3 implies that nine spin-rotation constants in each of the \tilde{B} and \tilde{X} states need to be determined. However, it was shown by Brown and Sears²⁴ that only six can be determined in the general case of a molecule with C_1 symmetry. Fewer can be determined for higher symmetry, for example, only four can be determined for a molecule with C_s symmetry.

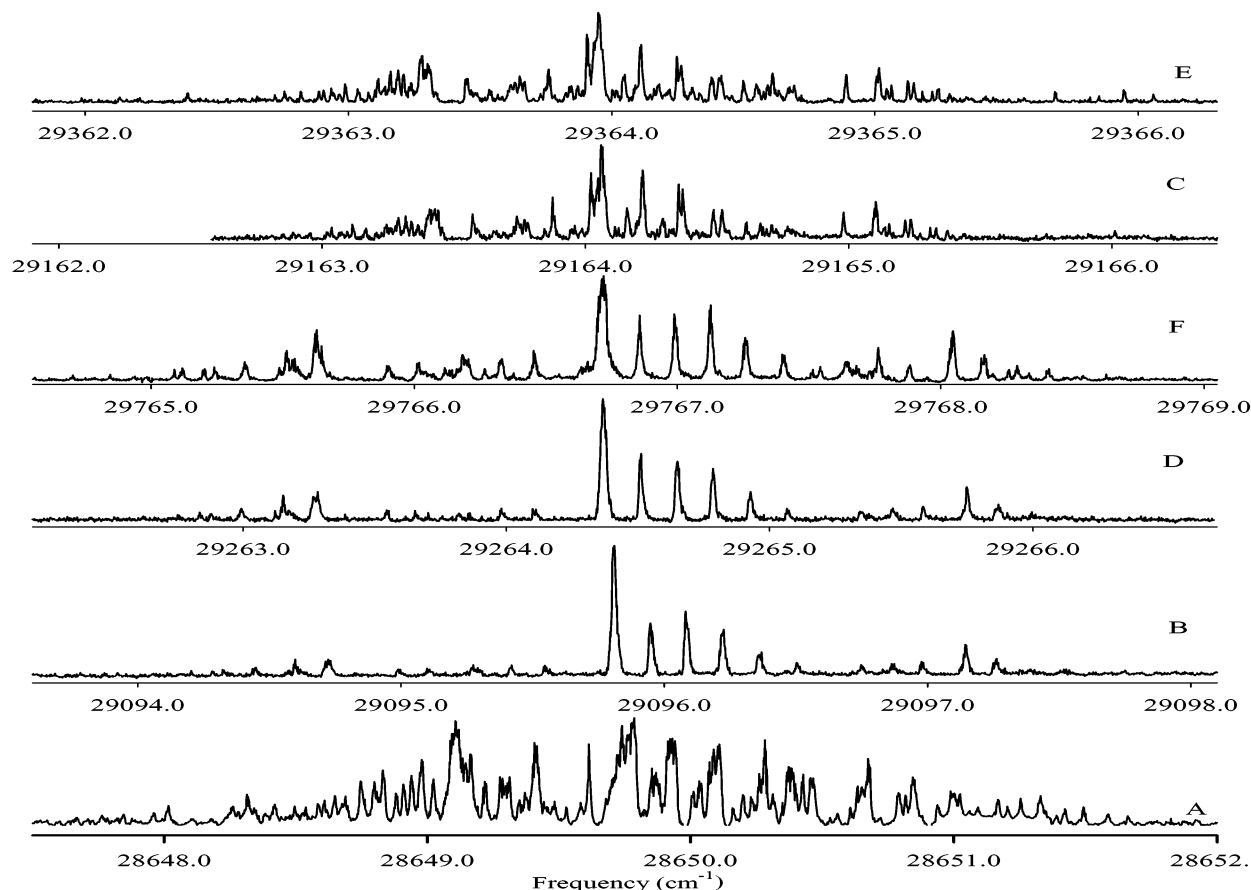


Figure 2. Rotationally resolved spectra of bands A through F in 1-butoxy.

In the general case, the spin-rotation constants that can be determined for a single isotopic species are given below in terms of their relationship to the components of the reduced spin-rotation tensor $\tilde{\epsilon}$ introduced by Brown and Sears:²⁴

$$T_0^0(\tilde{\epsilon}) = (-1/\sqrt{3})(\tilde{\epsilon}_{aa} + \tilde{\epsilon}_{bb} + \tilde{\epsilon}_{cc}) = \sqrt{3}a_0 \quad (4)$$

$$T_0^1(\tilde{\epsilon}) = (-1/\sqrt{2})i(\tilde{\epsilon}_{cb} - \tilde{\epsilon}_{bc}) = 0 \quad (5)$$

$$T_{\pm 1}^1(\tilde{\epsilon}) = (1/2)[(\tilde{\epsilon}_{ba} - \tilde{\epsilon}_{ab}) \pm (\tilde{\epsilon}_{ca} - \tilde{\epsilon}_{ac})] = 0 \quad (6)$$

$$T_0^2(\tilde{\epsilon}) = (1/\sqrt{6})(2\tilde{\epsilon}_{aa} - \tilde{\epsilon}_{bb} - \tilde{\epsilon}_{cc}) = -\sqrt{6}a \quad (7)$$

$$T_{\pm 1}^2(\tilde{\epsilon}) = \pm(1/2)[(\tilde{\epsilon}_{ba} + \tilde{\epsilon}_{ab}) \pm (\tilde{\epsilon}_{ca} + \tilde{\epsilon}_{ac})] = \pm(d \pm ie) \quad (8)$$

$$T_{\pm 2}^2(\tilde{\epsilon}) = (1/2)[(\tilde{\epsilon}_{bb} - \tilde{\epsilon}_{cc}) \pm (\tilde{\epsilon}_{bc} + \tilde{\epsilon}_{cb})] = (b \mp ic) \quad (9)$$

The parameters a_0 , a , b , c , d , and e were defined by Raynes²⁵ and because of their convenience in notation are used in our spectral analysis. In the case of our experiments on the alkoxy radicals, spin-rotation coupling is only expected to be large enough to be observed in the \tilde{X} state because of the presence of the low-lying, quasi-degenerate \tilde{A} state. Contributions from higher electronic states can be neglected²⁶ for the \tilde{X} state constants, and any spin-rotation splittings in the \tilde{B} state are expected to be too small to resolve because of an absence of any quasi-degenerate states.

4. Quantum Chemistry Computations and Predicted Conformers and Molecular Parameters

Quantum chemistry calculations of the rotational and spin-rotation constants were performed²⁶ to serve as a guide in the

fitting procedure. In our work on 1-propoxy, we demonstrated that such predictions are invaluable in making correct line assignments and eventually fitting the spectra. The predictions assume an even greater significance for the more complex spectra of 1-butoxy and 1-pentoxy for which numerous conformers exist. To predict the molecular constants of the different conformers of the 1-butoxy and 1-pentoxy radicals, we first need to understand the conformational isomerism in these two species.

4.1. Conformers of 1-Butoxy and 1-Pentoxy. The general method for analytically determining the number of conformers of the primary alkoxy radicals has already been described in our 1-propoxy paper¹⁷ and can be extended to 1-butoxy and 1-pentoxy. In 1-butoxy, there are two pairs of three-bond sets, that is, C_2-C_1-O with $C_1-C_2-C_3$ and $C_1-C_2-C_3$ with $C_2-C_3-C_4$ that can form two dihedral angles, ϕ_1 and ϕ_2 , illustrated in the Newman diagrams of Figure 5a. If we consider the first structure shown in Figure 5a, which has C_s symmetry as a reference structure, then rotation about the C_1-C_2 bond changes the value of the angle ϕ_1 with three values expected to correspond to staggered minima, as shown in the first row of Figure 5a. The three structures are designated T_1 , G_1 , and G_1' , respectively, for trans, gauche clockwise, and gauche counterclockwise for the C_1-C_2 torsion. We can also rotate about the C_2-C_3 bond to obtain different values of the angle ϕ_2 with again three staggered minima expected, as shown in the second row of Figure 5a. These are analogously designated T_2 , G_2 , and G_2' for the C_2-C_3 torsion. Because the values of ϕ_1 and ϕ_2 are independent, they can be combined to form a total of nine conformers. The conformer corresponding to T_1T_2 has C_s symmetry and is unique. Of the remaining eight conformers, four are unique and the others are their mirror images (indicated in parentheses), that is, T_1G_2 (T_1G_2'), G_1T_2 (G_1T_2'), G_1G_2

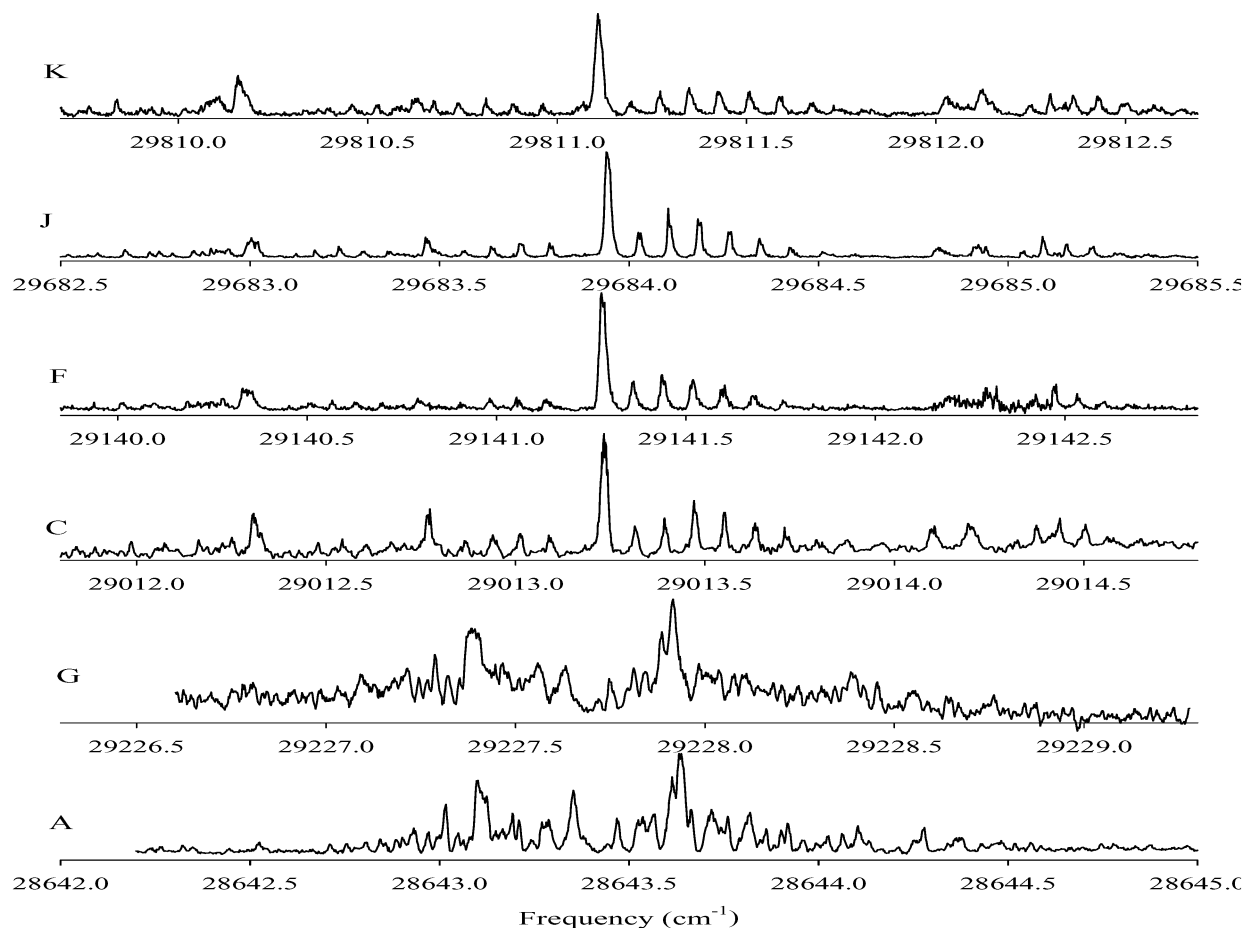


Figure 3. Rotationally resolved spectra of bands A, G, C, F, J, and K of 1-pentoxy.

($G_1'G_2'$), and $G_1'G_2$ (G_1G_2'). The unique conformers are pictured in Figure 5b.

By induction, one can arrive at the following empirical formula to determine the number of distinguishable conformations (N) for the primary alkoxy radicals:

$$N = \frac{3^{n-2} - 1}{2} + 1 \quad (10)$$

where n is the number of carbon atoms. To rationalize eq 10, we note that there are $n - 2$ possible dihedral angles that can be combined. These angles have minima at three possible values. Thus, the total number of possible conformations is 3^{n-2} . Of these, half of the conformers (other than the C_s one) are mirror images and thus indistinguishable. Thus, the total number of distinguishable conformers is given by eq 10.

We can carry out the same exercise for 1-pentoxy in which there are three torsional angles and, hence, $3^3 = 27$ possible conformers of which only 14 are distinguishable in accordance with eq 10. These are as follows: $T_1T_2T_3$, $G_1T_2T_3$ ($G_1'T_2T_3$), $T_1T_2G_3$ ($T_1T_2G_3'$), $G_1T_2G_3$ ($G_1'T_2G_3'$), $T_1G_2T_3$ ($T_1G_2'T_3$), $G_1T_2G_3'$ ($G_1'T_2G_3$), $G_1G_2'T_3$ ($G_1'G_2T_3$), $T_1G_2G_3'$ ($T_1G_2'G_3$), $G_1G_2'G_3$ ($G_1'G_2G_3'$), $G_1G_2T_3$ ($G_1'G_2'T_3$), $G_1G_2G_3'$ ($G_1'G_2'G_3$), $T_1G_2G_3$ ($T_1G_2'G_3'$), $G_1G_2G_3$ ($G_1'G_2'G_3'$), $G_1'G_2G_3$ ($G_1G_2'G_3'$). The 14 unique conformers of 1-pentoxy are pictured in Figure 6.

4.2. Prediction of Rotational and Spin-Rotation Constants.

Details of the procedures and calculations of the rotational and spin-rotation constants can be found elsewhere.²⁶ Only a brief summary will be given here. Rotational constants were determined by analytic geometry optimization at the B3LYP/6-

31+G* and the CIS/6-31+G* levels for the \tilde{X} and \tilde{B} states, respectively. The calculations were performed using the Gaussian 98 package.²⁷ A semiempirical approach based upon the knowledge of the experimentally determined spin-rotation constants of the ethoxy radical was used to estimate the spin-rotation constants.²⁶

5. Results—1-Butoxy

The calculated molecular constants of the five unique conformers of 1-butoxy are given in brackets in Table 1. Using these constants, we simulated the $\tilde{B}-\tilde{X}$ transitions of all five conformers, and the results are shown in Figure 7. It is evident from Figure 7 that the rotational structure of all the five conformers should be distinguishable. The experimental spectra can be compared with these simulations to find the best match for the initial guess for the fit. A comparison of Figures 2 and 7 shows that the simulation using the calculated constants of conformer G_1T_2 appears to be the best candidate for the spectrum of band A. The rotational constants of conformer T_1T_2 are rather unique, and there is little doubt that the conformational assignment for band B (as well as bands D and F) is conformer T_1T_2 . Finally, it is clear that the best candidate for band C (and E) is conformer T_1G_2 .

The full rotational analysis of the bands A through F was carried out in a similar manner as in the case of 1-propoxy to confirm the above conformational assignments and obtain structural information. The rotational analysis of several bands of 1-butoxy will be described in detail to serve as an example of the method of analysis used to fit the rotationally resolved spectra of the vibronic bands.

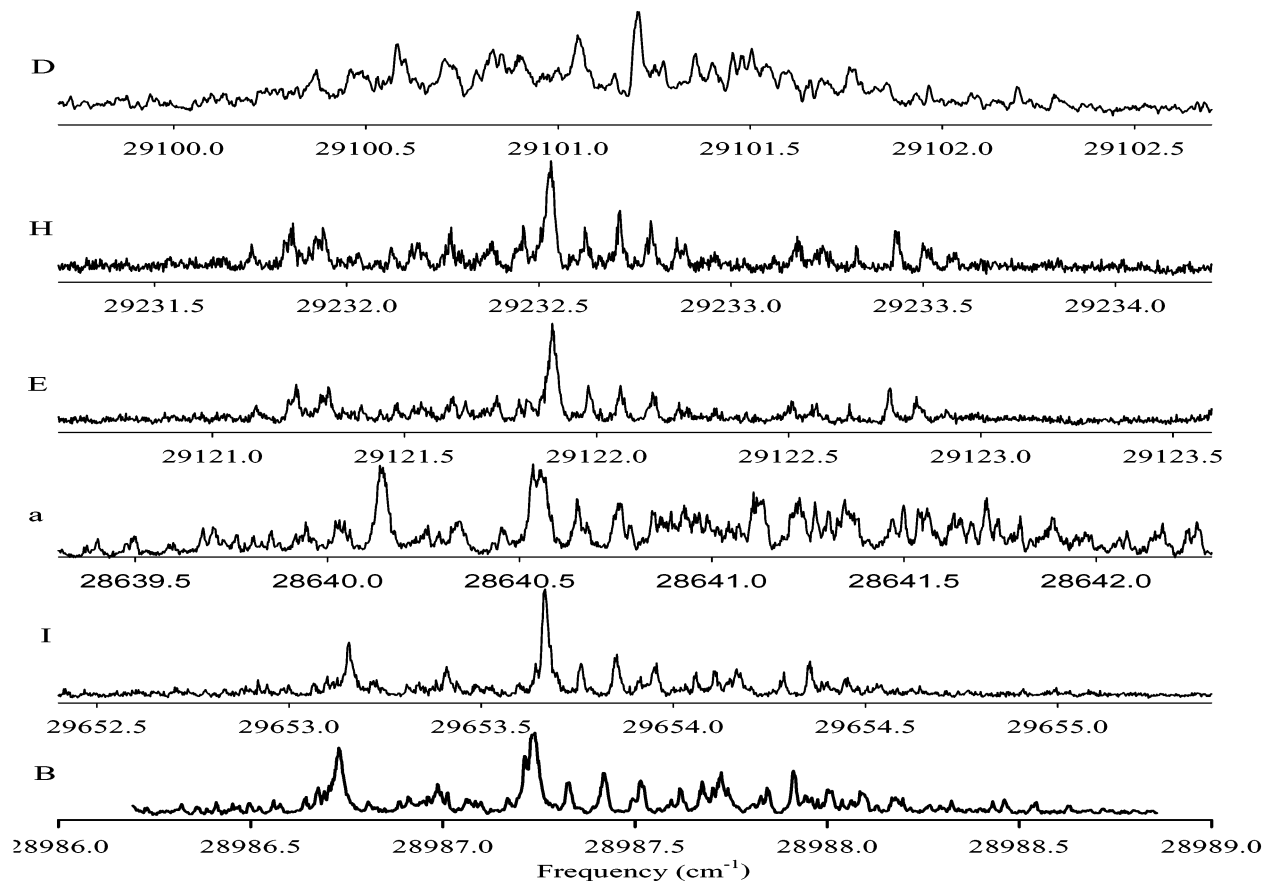


Figure 4. Rotationally resolved spectra of bands B, I, a, E, H, and D of 1-pentoxy.

5.1. 1-Butoxy—Band B. *5.1.1. Rotational Structure.* It is clear from Figures 2 and 7 that the most likely conformational assignment for band B (and bands D and F) of 1-butoxy is conformer T_1T_2 , which has C_s symmetry. As expected for a C_s symmetry molecule, the spectrum of band B is quite simple; pure c-type transitions are observed and P, Q, and R branches can be clearly distinguished. This band is analogous, in terms of rotational structure, to band B of 1-propoxy of which the carrier was likewise shown to be a C_s trans conformer.¹⁷ In that work, we demonstrated that all six rotational constants can be determined, in principle, from the spectra, and a similar argument holds for 1-butoxy. As suggested by Table 1, all conformers of 1-butoxy are near-prolate symmetric tops. Thus, it is reasonable that line assignments and approximate selection rules for the rotational transitions were made assuming symmetric top quantum numbers.

5.1.2. Spin Rotation. To fit the spectrum and obtain structural information therefrom, one also has to consider the effect of spin rotation on the spectrum. For conformer T_1T_2 of 1-butoxy, only four spin-rotation constants can be determined²⁴ because for a molecule with C_s symmetry the constants c and e vanish. Furthermore, the constant $\tilde{\epsilon}_{cc} = 0$ unless contributions to the spin-rotation tensor from excited electronic states²⁶ other than \tilde{A} are considered. However, these contributions will be so small that it is unlikely that they will be detected by our experiment. As shown in our work on 1-propoxy, there are specific linear combinations of the diagonal components of the spin-rotation tensor that cause certain transitions to split. Transitions involving $K'' = 0$ are split by the amount $(N'' + 1/2)(a_0 - a)$, while those involving $K'' = \pm 1$ and $N'' = 1$ are split by the amount $3/2(a_0 + a/2)$. Using the calculated values of these constants, we may predict the magnitude of the spectral splittings to serve as a

guide in making assignments. The constants a_0 and a are diagonal in K'' and should thus be well determined from the spectrum. The constant b mixes levels with $\Delta K'' = \pm 2$, which will be strongly mixed by asymmetric top terms and should thus be determined as well. Thus, we should be able to well determine all three unique components of the spin-rotation tensor from the spectrum.

5.1.3. Fit. To complete the line assignments, it is important to identify all of the spin-rotation splittings. The calculated value of the spin-rotation constant $(a_0 + a/2)$ is large (2.1 GHz), and it was fairly trivial to identify spin-rotation splittings caused by this constant. These splittings are shown in Figure 8. However, the calculated value of the constant $(a_0 - a)$ is quite small (0.12 GHz). Thus, the effect of this constant on the spectrum is much less, although it can still be determined from the spectrum as demonstrated in Figure 9. The $K'' = 0$ transitions (which are affected uniquely by this spin-rotation constant) are barely split (they look broadened rather than split). However, the effect of this spin-rotation constant on the spectrum is still observable for the high N'' ($N'' > 2$) transitions as shown in Figure 9. Furthermore, this constant will have a small effect on the splitting of the $N'' \neq 0, K'' = 0 \leftrightarrow |K''| = 1$ transitions and thus can be well determined. The simulated fit spectrum of band B from the fit constants is shown in Figure 10B.

The vibrationally excited bands D and F were fit independently. The ground-state constants obtained from the fits of all three bands (B, D, and F) were found to be the same within two standard deviations. The resulting constants for the vibrationless levels of the \tilde{X} and \tilde{B} states of conformer T_1T_2 are given in Table 1. The ground-state constants reported are those

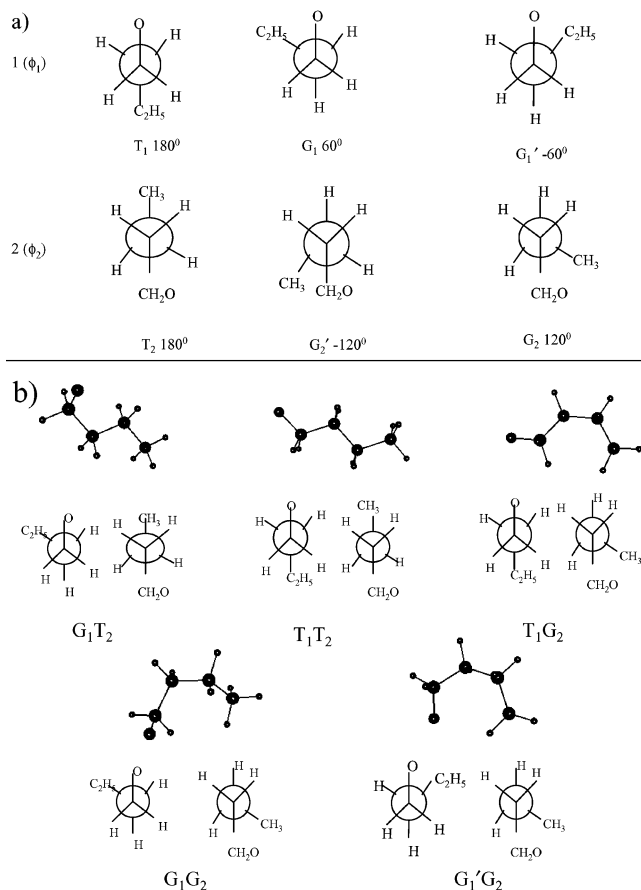


Figure 5. Values (a) for 1-butoxy of the dihedral angles ϕ_1 and ϕ_2 (staggered) for which local minima occur and structures (b) of five unique conformers of 1-butoxy corresponding to the combination of angles ϕ_1 and ϕ_2 at their local minima.

obtained by weighting the constants obtained from the fits of the bands by the inverse of the respective standard deviations of the fit.

5.2. 1-Butoxy—Band A. **5.2.1. Rotational Structure.** It has been postulated that the likely assignment for band A is conformer G_1T_2 upon the basis of the good agreement between the simulation of the $\tilde{B}-\tilde{X}$ transition using the calculated molecular constants of conformer G_1T_2 and the experimental spectrum of band A (see Figures 7 and 2). The spectrum is therefore expected to have fairly complicated rotational structure. Conformer G_1T_2 of 1-butoxy is analogous to the gauche conformer (G) of 1-propoxy, which has been discussed in detail previously.¹⁷ Conformer G_1T_2 has C_1 symmetry, and thus transitions will be allowed by all three components of the electric dipole moment.

5.2.2. Spin Rotation. Because conformer G_1T_2 has only C_1 symmetry, six components of the spin-rotation tensor need to be determined. The constants a , a_0 , and b should be well determined from the experimental spectrum as discussed in the case of band B. The effect of the spin-rotation constants d and e , which are off-diagonal in K'' , should be smaller; however, their effect should increase with increasing N'' . The constant c mixes states with $\Delta K' = \pm 2$, that is, the same states that are mixed by the asymmetric part of the rotational Hamiltonian and should thus be determinable from the spectrum.

5.2.3. Fit. The simulated spectrum shown in Figure 7a was used as the starting point in the analysis of band A. It is quite clear that the overall correlation between the experimental spectrum and the simulation is quite good. This implies that

the calculated molecular constants used to generate the simulation are rather close to the experimental values. However, to carry out a fit to obtain the molecular constants, it is necessary to identify spin-rotation effects in the spectrum to make the correct line assignments. In the following analysis, line assignments were made upon the basis of the good correspondence between the simulated and experimental spectra.

It is easier to pick out splittings in the high N'' transitions (extremes of the spectrum) because the splitting increases with increasing N'' . This is demonstrated in Figure 11. Figure 11a shows a simulation using calculated rotational constants only with no spin rotation. Clearly, the transitions shown using the solid lines appear to be split. The splitting indeed occurs upon adding the calculated values of all of the spin rotation constants, as can be seen in Figure 11b. The assignments shown in Figure 11b using the solid lines were made to fit one linear combination of the rotational constants in the excited state to yield the improved simulation shown in Figure 11c. The relative weights of the a , b , and c transition dipole moments were varied (from their ab initio values) to get better relative intensities.

The effect of the diagonal components of the spin-rotation tensor, namely, $(a_0 + a/2)$ and $(a_0 - a)$ is illustrated in Figure 12. The assignments shown are those corresponding to $|K'| = 1 \leftrightarrow K'' = 0$ transitions in a Q-branch and $K' = 0 \leftrightarrow |K''| = 1$ transitions in another Q-branch. By making these assignments in addition to those already made in Figure 11, more linear combinations of the rotational constants can be fit as shown in the simulation 12c, obtained by fitting all three linear combinations in the ground state. This simulation clearly looks closer to the experimental spectrum than the simulation in 12b. We can then make the additional assignments shown in Figure 12c and in other parts of the spectrum as well to progressively fit all of the linear combinations of the rotational constants in the excited state as shown in Figure 12d. It is evident that this simulation resembles the experimental spectrum even more. Thus, by progressively refining the rotational constants, we can make more and more assignments unambiguously. Then one can fit the diagonal components of the spin-rotation tensor, namely, $(a_0 + a/2)$, $(a_0 - a)$, and b (of which the effect on the spectrum is the greatest of all the spin-rotation constants) to obtain simulation 12e. At this stage, approximately 130 assignments could be made and all of the rotational constants and five spin-rotation constants ($(a_0 + a/2)$, $(a_0 - a)$, b , d , and c) could be fit to yield simulation 12f.

In the final fit, all rotational and spin-rotation constants were determined. The resulting simulation spectrum of band A is shown in Figure 10A and the results of the fit are given in Table 1.

5.3. 1-Butoxy—Band C. Conformer T_1G_2 of 1-butoxy also has C_1 symmetry, and thus six rotational and six spin-rotation constants should again be obtainable from the spectrum. The resulting fit spectrum is shown in Figure 10C. The vibrationally excited band E was also independently fit to obtain the molecular constants of this conformer. A comparison of the fits of bands C and E revealed that the ground-state constants were all within two standard deviations. Thus, following the same procedure as that described for conformer T_1T_2 , we inversely weighted the ground-state constants by the corresponding standard deviation and took an average. The molecular constants of the \tilde{X} and \tilde{B} states are given in Table 1.

6. Results—1-Pentoxy

Although somewhat more complicated, the analysis of the rotational structure of the bands of 1-pentoxy, shown in Figures

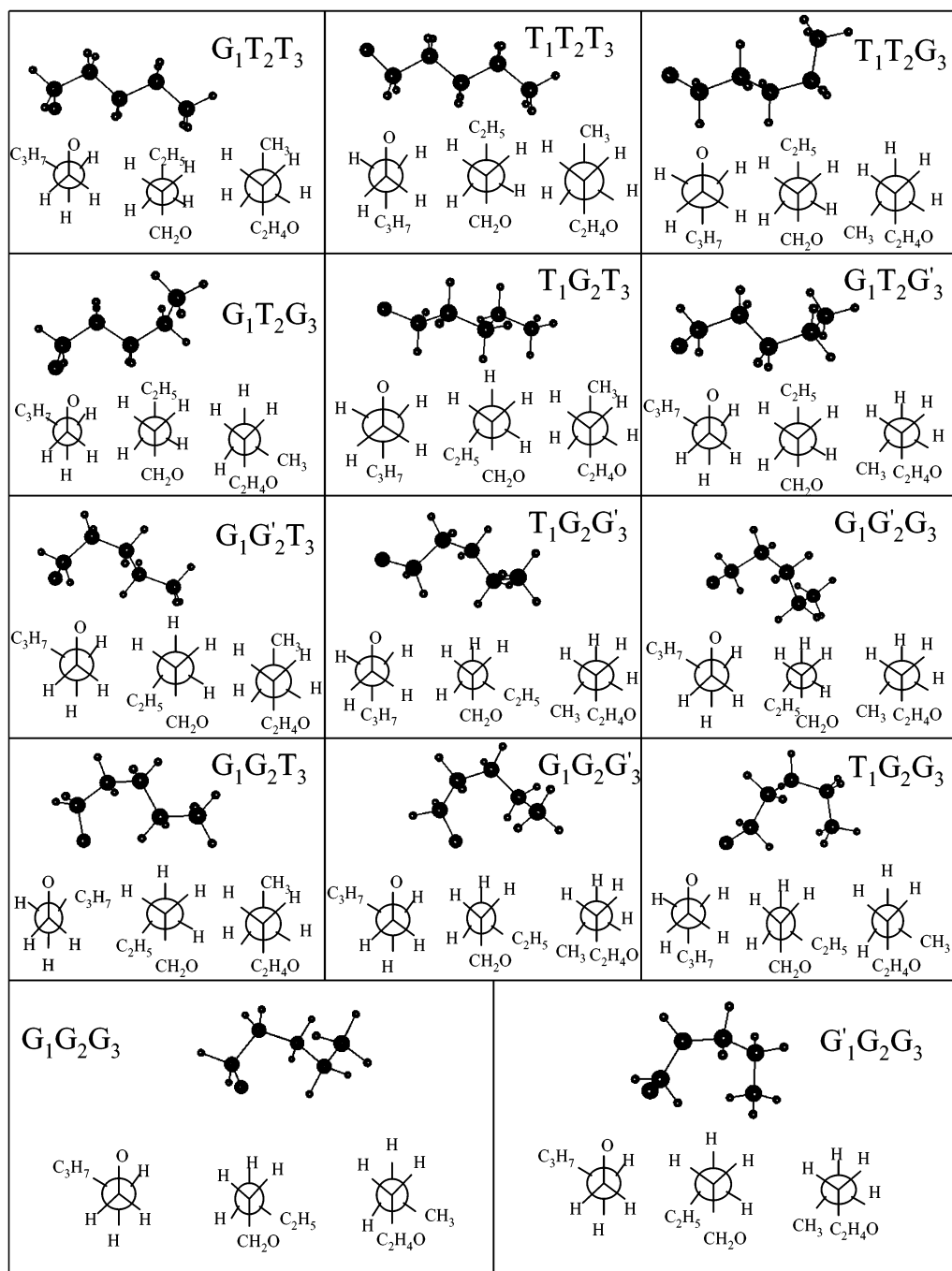


Figure 6. Structures of 14 unique conformers of 1-pentoxy at their local minima. The corresponding Newman projections are also shown.

3 and 4, proceeded very much along the same lines as that for the bands of 1-butoxy. We present the results of that analysis here and give the details (and supporting spectra and simulations) in the Supporting Information for this article.

The bands in Figures 3 and 4 fall into six distinct groups, (A, G), (B, I), (C, F, J, K), (D), (E, H), and (a), which correspond to different conformers. In all cases, except for band D, good simulations of the observed band structure were obtained using fit values of the molecular parameters quite similar to those calculated for one of the 14 conformers. These fit and calculated parameters are summarized in Table 2. (For calculated molecular parameters of all 14 conformers, see ref 26.) Because of the relatively low *S/N* for band D, a rigorous rotational/fine-structure analysis could not be performed nor a unique conformer assignment made.

7. Discussion

7.1. Vibrational Assignments. *7.1.1. 1-Butoxy.* Table 1 indicates that both the rotational and spin-rotation constants are important parameters in establishing the conformational identity of the carrier of the spectrum. For instance, conformers G_1T_2 and T_1G_2 have rotational constants differing by $\leq 8\%$, while the spin-rotation constants differ by $\geq 70\%$. However, the calculated and experimental rotational constants for a particular conformer given in Table 1 agree to within 3%, a similar trend being observed in the spin-rotation constants, although the reliability of their predictions is significantly lower.²⁶ Clearly, the rotational and fine structure of a given vibrational band unambiguously “bar-codes” for the conformer carrying that band. The results of the fits of the vibronic bands A through E

TABLE 1: Experimentally Determined and Calculated Molecular Constants from Spectral Bands of 1-Butoxy^a

const (GHz)	band A [G ₁ T ₂] 124 lines assigned $\sigma = 79$ MHz	band B [T ₁ T ₂] 79 lines assigned $\sigma = 51$ MHz	band C [T ₁ G ₂] 223 lines assigned $\sigma = 60$ MHz	...[G ₁ G ₂][G ₁ 'G ₂] ...
A''	13.419(6) [13.53]	20.19(2) [20.12]	12.42(1) [12.40]	... [8.90]	... [7.57]
B''	2.397(2) [2.34]	2.044(6) [2.00]	2.443(2) [2.41]	... [2.89]	... [3.65]
C''	2.240(2) [2.19]	1.934(4) [1.90]	2.242(1) [2.21]	... [2.69]	... [2.75]
$\tilde{\epsilon}_{aa}''$	-1.09(2) [-1.13]	-5.71(4) [-5.47]	-4.31(2) [-3.99]	... [-0.75]	... [-0.08]
$\tilde{\epsilon}_{bb}''$	-0.53(3) [-0.54]	-0.25(2) [-0.15]	-0.006(9) [0.00]	... [-0.29]	... [-1.18]
$\tilde{\epsilon}_{cb}''$	-0.13(1) [-0.08]	0.00 [0.00]	-0.050(8) [-0.06]	... [-0.45]	... [-0.05]
$ \tilde{\epsilon}_{ab}'' = \tilde{\epsilon}_{ba}'' $	0.69(5) [1.10]	0.64(4) [1.60]	0.00 [0.00]	... [0.53]	... [0.30]
$ \tilde{\epsilon}_{bc}'' = \tilde{\epsilon}_{cb}'' $	0.15(5) [0.20]	0.00 [0.00]	0.00 [0.00]	... [0.36]	... [0.23]
$ \tilde{\epsilon}_{ac}'' = \tilde{\epsilon}_{ca}'' $	0.40(5) [0.43]	0.00 [0.00]	0.59(4) [0.68]	... [0.68]	... [0.07]
A'	11.821(3) [12.33]	18.07(1) [18.56]	12.64(1) [12.73]	... [8.18]	... [7.51]
B'	2.462(1) [2.42]	2.049(3) [2.02]	2.331(5) [2.35]	... [3.02]	... [3.46]
C'	2.247(1) [2.19]	1.916(3) [1.90]	2.183(4) [2.21]	... [2.69]	... [2.75]
T ₀₀	28649.47(1)	29095.28(1)	29163.73(1)
relative energies ^b	... [0.0]	... [7]	... [424]	... [344]	... [423]

^a In brackets, we indicate the conformer assignments and the corresponding values of the molecular parameters predicted from the quantum chemistry calculations. Experimental ground-state constants were obtained by averaging over all of the vibrational bands observed for a particular conformer weighted inversely by the standard deviation of the fit, σ . The excited-state constants are those corresponding to the vibrationless level obtained from the fits of the origin bands A, B, and C for the three conformers. The rotational constants of the vibrationally excited states obtained from the fits of bands D and F for conformer T₁T₂ are A' = 18.51(1), B' = 2.043(4), C' = 1.934(4), T_{0D} = T₀₀ + 168.55(1) cm⁻¹ and A' = 17.996(6), B' = 2.018(2), C' = 1.916(2), T_{0F} = T₀₀ + 670.91(1) cm⁻¹, respectively, and those of band E for conformer T₁G₂ are A' = 12.635(2); B' = 2.331(2); C' = 2.183(3); T_{0E} = T₀₀ + 199.83(1) cm⁻¹. The calculated constants of the assigned conformers (of which the calculated values most closely match the experimental ones) are given in brackets. The error quoted for the constants is one standard deviation. Ellipsis points indicate that corresponding experimental data is not available. ^b Relative energies (cm⁻¹) are for the \tilde{X} state.

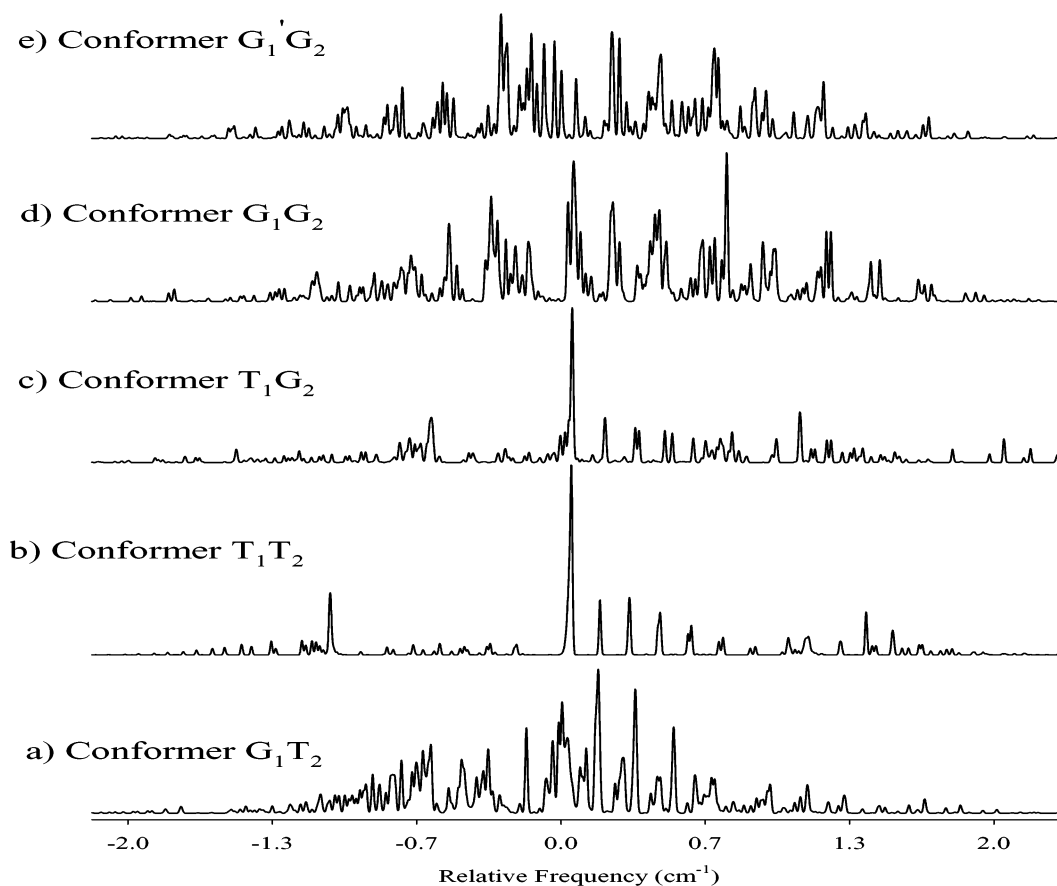


Figure 7. Simulations of the $\tilde{B}-\tilde{X}$ transitions of the five conformers of 1-butoxy using calculated rotation and spin-rotation constants. The calculated values of the square of the transition dipole moments $a:b:c$ used to obtain the simulations are 17:1:8, 0:0:1, 1:14:13, 1.5:1:2.6, and 1:0:1.5 for simulations a–e, respectively.

of 1-butoxy collected in Table 1 firmly establish the presence of three different conformers and identify the bands associated with each.

Conformer G₁T₂ has only one band (band A) bearing its rotational bar code. It is reasonable to consider this band as the origin of the $\tilde{B}-\tilde{X}$ transition because a search for other bands, up to 1000 cm⁻¹ to the red of band A, yielded no signal.

Likewise, no excited vibrational bands of conformer G₁T₂ could be identified, although it is evident from Figure 1a that there are a few bands, other than A–E, that are too weak to rotationally resolve and classify according to conformer.

Conformer T₁T₂ of 1-butoxy, which is analogous to the trans (T) conformer of 1-propoxy, has three vibrational bands, the lowest of which (band B) is assumed to be the origin. Band F

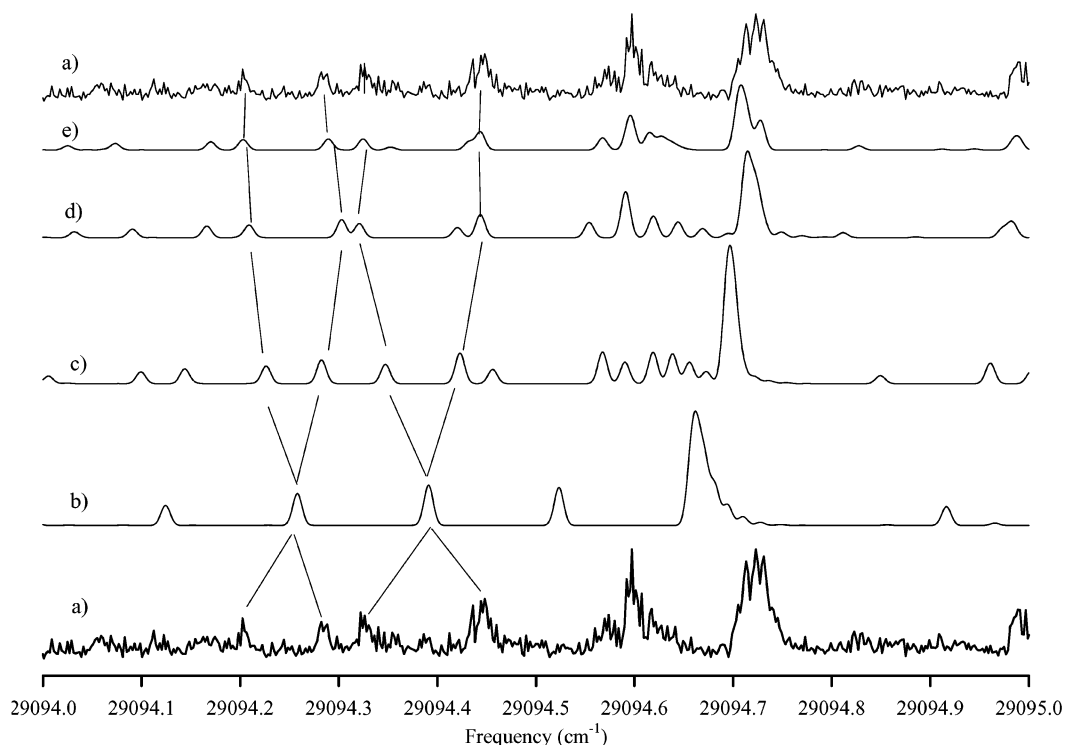


Figure 8. Low-frequency end (a) of the experimental spectrum of band B, (b) simulation of the $\tilde{B}-\tilde{X}$ transition of T_1T_2 conformer of 1-butoxy (relative intensity of dipole components, $a:b:c = 0:0:1$, and the rotational temperature is 1.2 K), (c) addition of calculated value of one spin-rotation constant ($a_0 + a/2$) that splits transitions with $|K''| = 1$, (d) simulation after fitting two linear combinations of the rotational constants, and (e) simulation after fitting five linear combinations of the rotational constants and the spin-rotation constant ($a_0 + a/2$).

at 672 cm^{-1} is the only one in the C–O stretch region; its frequency is also in reasonably good agreement with ab initio calculations,²⁶ which, while not particularly accurate for the \tilde{B} state, are qualitatively useful in making vibrational assignments. As per the calculations, the remaining strong band D is assigned to a low-frequency C–C–O backbone bend or deformation.

Finally, for conformer T_1G_2 , we have two lines with the lowest one (C) assumed to be the origin. Band E at 200 cm^{-1} is assigned as a C–C–O backbone deformation, which is in good agreement with ab initio calculations. No band is detected in the C–O stretch region. The vibrational assignments for all of the 1-butoxy conformers are summarized in Table 3.

The LIF spectrum of each of the three conformers seems to end abruptly. (We have scanned 1500 cm^{-1} to the blue of band F and observed nothing.) The maximum spectral extent is $<700\text{ cm}^{-1}$ for conformer T_1T_2 , which alone contains one quantum of C–O stretch excitation, while the T_1G_2 and G_1T_2 conformer spectra terminate at even lower energies. A similar behavior was observed in the case of the analogous trans conformer of 1-propoxy¹⁷ in which the T conformer exhibits a single C–O stretch excitation and the G conformer spectrum terminated below this energy. This is in sharp contrast to the previously reported spectra of the smaller alkoxyes such as methoxy, ethoxy, and 2-propoxy in which the predominant feature of the spectra is a strong progression in the C–O stretch mode in the \tilde{B} state. Those LIF spectra terminated at $\geq 3000\text{ cm}^{-1}$ above the origin. In methoxy, the termination of the LIF spectrum is believed to be by predissociation from repulsive states asymptotically approaching the $R^* + O$ dissociation limit. In the case of 1-propoxy, the abrupt termination of the spectrum was attributed to rapid internal conversion to the \tilde{X} state that occurs upon vibrational excitation,¹⁷ an explanation that likely accounts for the similar behavior in 1-butoxy.

7.1.2. 1-Pentoxy. Table 2 shows that the calculated and experimentally determined rotational constants for each of the five observed conformers of 1-pentoxy agree to $<3\%$, while the rotational constants of the different conformers differ by as much as 70%. A comparable statement can be made about the spin-rotation constants, although the predictions are poorer than those for the rotational constants (as expected given the semiempirical model used to calculate the former, ref 26). Thus, we conclude that the carriers of the spectral bands *a* through *K* of 1-pentoxy can be uniquely assigned to the five different conformers.

The vibrational assignments for the bands are summarized in Table 3. It is clear from this table that, as in the case of 1-propoxy and 1-butoxy, a maximum of only one quantum of C–O stretch excitation is observed (all bands other than *a* through *K* are too weak to rotationally resolve and assign). This abrupt termination of the LIF spectra of the different conformers is again likely attributable to rapid internal conversion upon vibrational excitation in the \tilde{B} state.

7.2. Electronic Origins. **7.2.1. 1-Butoxy.** The lowest frequency origin band is that of conformer G_1T_2 (band A), which is shifted -446 cm^{-1} with respect to that of conformer T_1T_2 , while the origin of conformer T_1G_2 is shifted $+68\text{ cm}^{-1}$ with respect to the same reference. As Table 1 indicates, according to our ab initio calculations, the lowest energy conformer is conformer G_1T_2 , while conformer T_1T_2 is only 7 cm^{-1} higher. If we consider conformer T_1T_2 as a reference, then this implies that the \tilde{B} state of conformer G_1T_2 is stabilized by $\geq 400\text{ cm}^{-1}$ and the \tilde{B} state of conformer T_1G_2 is destabilized by $\geq 50\text{ cm}^{-1}$ as compared to the \tilde{B} state of conformer T_1T_2 . We can rationalize this observation as follows. In the case of conformer G_1T_2 , the stabilization may be attributed to a nonclassical C–H \cdots O hydrogen bond, which is more important in the \tilde{B} state because of the larger volume of the doubly occupied p-orbitals

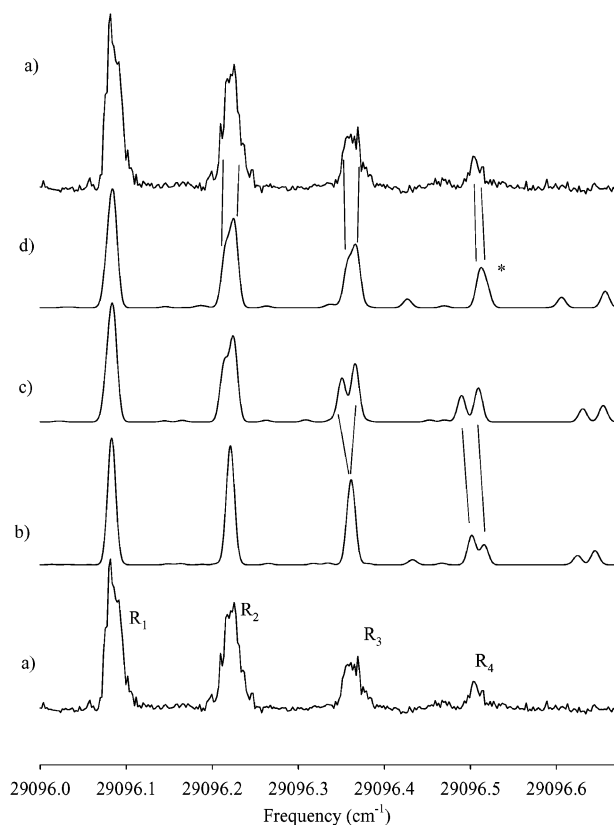


Figure 9. Portion of (a) experimental spectrum of band B of 1-butoxy, (b) simulation of the $\tilde{B}-\tilde{X}$ transition of T_1T_2 conformer showing the $|K'| = 1 \leftrightarrow K'' = 0$ R branch transitions using a rigid-rotor Hamiltonian with no spin-rotation, (c) simulation upon adding the calculated value of the spin-rotation constant $a_0 - a$ (the splitting of the R_2 and R_3 transitions is noticeable), and (d) simulation after adding the calculated value of the spin-rotation constant d (the R_4 transition (marked with an asterisk), which was more split before adding this constant, looks more like the experimental transition due to the addition of this off-diagonal constant. Thus these two spin-rotation constants can be determined from this portion of the spectrum).

on the oxygen atom. A similar observation was made in the analogous gauche conformer of 1-propoxy.¹⁷ This kind of hydrogen bonding is not possible in the other two conformers, which have local C_s symmetry around the oxygen atom. It is probable that the conformer T_1G_2 is destabilized because of steric repulsion between the end hydrogens in both the \tilde{X} and \tilde{B} states as compared to the \tilde{X} and \tilde{B} states of conformer T_1T_2 . The additional small destabilization (≥ 50 cm^{-1}) of the \tilde{B} state may be due to a small increase in the electron density on the C_α hydrogen atoms in the \tilde{B} state, which leads to an increase in the steric repulsion.

7.2.2. 1-Pentoxy. It is interesting to note that the electronic origins of the five observed conformers of 1-pentoxy fall into two broad groups depending on whether the local symmetry around the oxygen atom is C_s . The origins of conformers $G_1T_2T_3$ and $G_1T_2G_3$ in which the oxygen atom is rotated out of plane are almost identical at $\sim 28\,640$ cm^{-1} , whereas the origins of conformers $T_1T_2T_3$, $T_1T_2G_3$, and $T_1G_2T_3$, which have local C_s symmetry, are higher by 370, 347, and 482 cm^{-1} respectively. Likewise for 1-butoxy, the origin band of the corresponding “oxygen out-of-plane” conformer was lower by 446 cm^{-1} as compared to the C_s conformer, and this difference was attributed to the stabilization of the \tilde{B} state of the former due to $C-H\cdots O$ hydrogen bonding. Clearly, this trend continues in 1-pentoxy as well. The origins of conformers $T_1T_2T_3$ and $T_1T_2G_3$ differ by only 26 cm^{-1} , which implies that both the \tilde{X} and \tilde{B} states of

conformer $T_1T_2G_3$ are shifted by practically identical amounts with respect to the same states of the C_s conformer ($T_1T_2T_3$). This is reasonable because conformers $T_1T_2T_3$ and $T_1T_2G_3$ differ only in that the latter has the end ethyl group twisted out of the plane. Because it is quite far away from the oxygen chromophore, this should hardly effect the relative \tilde{B} and \tilde{X} state energies. On the other hand, the origin of conformer $T_1G_2T_3$ is higher than that of conformer $T_1T_2T_3$ by ~ 100 cm^{-1} . Conformer $T_1G_2T_3$ is analogous to conformer T_1G_2 of 1-butoxy in which the end ethyl group is rotated out of the plane, and a similar shift ($+68$ cm^{-1}) in the origin bands was observed. The destabilization of the \tilde{B} state of conformer $T_1G_2T_3$ of 1-pentoxy is likewise attributed to an increase in steric repulsion upon electronic excitation, as argued in the case of 1-butoxy.

7.3. Rotation and Spin-Rotation Constants. 7.3.1. 1-Butoxy.

Upon the basis of the good agreement between calculated and experimentally obtained rotational constants in both the \tilde{X} and \tilde{B} states, one can ascribe the geometry changes upon electronic excitation simply to be an increase in the C–O bond length and a decrease in the C–C–O bond angle, which is consistent with the large change in the C–O bonding character in the two states. Assuming this simple model, increases in the C–O bond length of 0.19, 0.20, and 0.19 Å and decreases in the C–C–O bond angles of 8.0°, 7.7°, and 7.8°, respectively, for conformers G_1T_2 , T_1T_2 , and T_1G_2 were deduced from the observed rotational constants.

The values for the components ($\tilde{\epsilon}_{\alpha\beta}$) of the spin-rotation tensor are given in Table 1, which indicates that the predicted spin-rotation constants agree relatively well with the experimentally determined ones. This further confirms that the simple semiempirical model used to predict the spin-rotation constants²⁶ is reasonable. This model assumes that the nature of the orbital carrying the unpaired electron does not change significantly from ethoxy to any other 1-alkoxy radical. Furthermore, as shown by Table 1, two conformers (G_1T_2 and T_1G_2) that have very similar rotational constants can be unambiguously distinguished from each other because of their very different predicted spin-rotation constants.

7.3.2. 1-Pentoxy. Table 2 indicates that the agreement between the calculated and experimentally determined rotation and spin-rotation constants of all five conformers is quite good. Indeed different conformers can be distinguished not only upon the basis of different rotational constants but also upon the basis of different spin-rotation constants, as illustrated by conformers $G_1T_2T_3$ and $T_1T_2G_3$. Upon the basis of the above simple model, one can deduce the changes in the C–O bond lengths and C–C–O bond angles from the rotational constants. The increases in the C–O bond length upon excitation for conformers $G_1T_2T_3$, $T_1T_2T_3$, $T_1T_2G_3$, $G_1T_2G_3$, and $T_1G_2T_3$ are, respectively, 0.19, 0.19, 0.16, 0.16, and 0.17 Å, and the concomitant decreases in the C–C–O bond angle are, respectively, 7.8°, 7.9°, 7.5°, 7.7°, and 7.7°.

7.4. Conformational Selectivity. It is well-known that at room temperature conversion among conformers is very facile. However, at the very low jet temperatures (< 1.5 K rotational temperatures), such interconversion is exceedingly unlikely on the time scale of the experiment. Presumably in the initial photolysis that produces the alkoxy radical there is sufficient energy to populate all (or at least most) of the possible conformers. (While there is sufficient energy in the photolysis to populate the various alkoxy conformers, there is no guarantee that this energy is randomized in the molecule. It is also possible that there is a propensity for the alkoxy conformer distribution to be determined by the conformational geometry of the alkyl

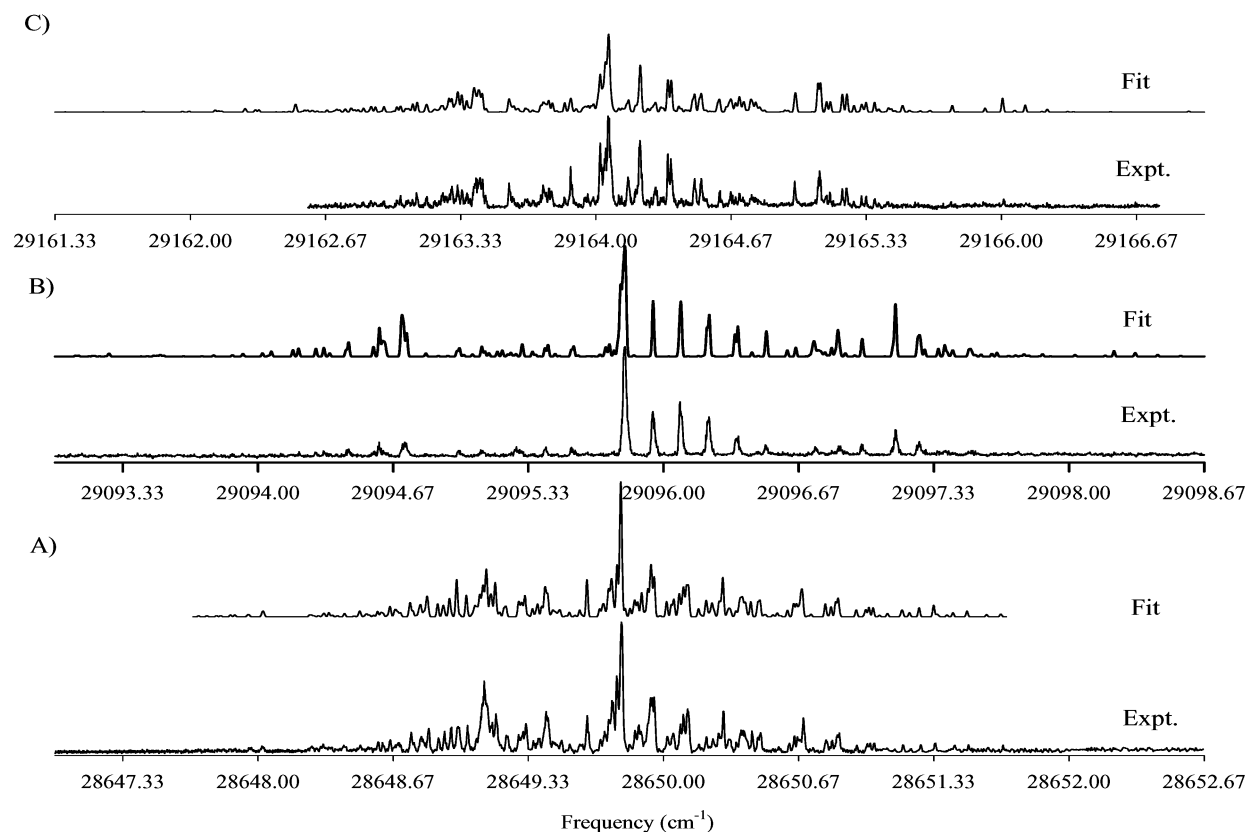


Figure 10. Comparison of experimental spectra with simulations based upon fit constants (Table 1) for (A) band A and G_1T_2 conformer, (B) band B and T_1T_2 conformer, and (C) band C and T_1G_2 conformer of 1-butoxy. For simulations A through C, the ratio of the electric dipole moments $a:b:c$ for the three bands are, respectively, 10:2:9, 0:0:1, and 3:7:7 (the calculated values are, respectively, 17:1:8, 0:0:1, and 1:14:13 for conformers G_1T_2 , T_1T_2 , and T_1G_2). The rotational temperatures are 1.2, 1.2, and 1.0 K, respectively.

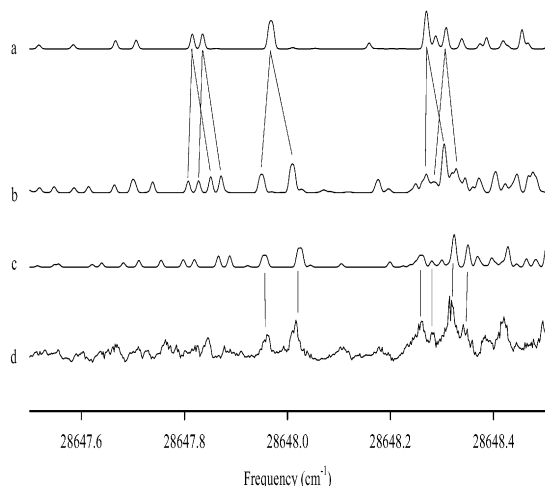


Figure 11. Spin-rotation in 1-butoxy conformer G_1T_2 : (a) simulation using calculated rotational constants without spin-rotation; (b) splitting of transitions upon adding the calculated values of all six spin-rotation constants; (c) fit of one linear combination of the rotational constants in the excited state; (d) experimental spectrum.

nitrite precursor. If we assume the precursor is at room temperature, a number of its conformations will be well populated but some of the higher energy ones will not. Following this argument, one might expect a clear preference for the lower-energy conformers of the alkoxy radicals. While the lowest-energy conformers do seem to be observed in all cases, there is seemingly a random-like sampling of the higher-energy conformers. For instance, in 1-butoxy, the two lowest-energy conformers (G_1T_2 and T_1T_2) are observed. The other

three conformers are all comparably and substantially higher in energy (from calculations $\sim 2kT$, where T is room temperature), yet only one, T_1G_2 , is observed.) As jet cooling takes place, many of the higher-energy conformers relax. However, clearly, equilibrium is not reached because at the low jet temperature only the lowest-energy conformer would be populated. Rather some conformers are “trapped” in higher-energy conformations. The question is then raised as to which conformers relax and which are trapped.

For 1-butoxy, we can compare Table 3 of the observed conformers with Figure 5, which shows the possible conformer structures. It is clear that two of the three observed conformers (G_1T_2 and T_1T_2) are of the straight chain variety. Of the three remaining conformers, only T_1G_2 is observed. It is interesting to note that the conformer $G_1G'_2$ closely resembles the cyclic transition state that converts 1-butoxy to the hydroxy butyl ($^{\bullet}CH-(CH_2)_2-CH_2OH$) radical, which would not be expected to be observable by LIF spectroscopy. The other unobserved conformer, G_1G_2 , differs from $G_1G'_2$ by only a 120° rotation of the O-containing methyl and might rapidly relax to $G_1G'_2$, which could be an effective sink for 1-butoxy radicals.

Similar, although somewhat less definitive, conclusions for 1-pentoxy can be reached by comparing Table 3 and Figure 6. We note that the five observed conformers are all straight-chain or nearly so. Furthermore, of this “category” of conformers (first two rows of Figure 6), only $G_1T_2G'_3$ has not been observed. Generally speaking, these conformers that have (or resemble) a cyclic structure (last three rows of Figure 6) have not been definitely observed (excluding one weak spectrum (D) of which assignment is uncertain). Of course, once again the transition state for the tautomerization reaction to produce the hydroxy

TABLE 2: Experimentally Determined and Calculated Rotational and Spin-Rotation Constants (in GHz) from Five Sets of Rotational Bands of 1-Pentoxy^a

const	band A [G ₁ T ₂ T ₃] 164 lines $\sigma = 52$ MHz	band C [T ₁ T ₂ T ₃] 79 lines $\sigma = 51$ MHz	band B [T ₁ T ₂ G ₃] 137 lines $\sigma = 71$ MHz	band a [G ₁ T ₂ G ₃] 103 lines $\sigma = 110$ MHz	band E [T ₁ G ₂ T ₃] 103 lines $\sigma = 117$ MHz
A''	9.66(2) [9.79]	16.30(2) [16.38]	9.65(1) [9.67]	7.932(6) [7.97]	10.56(2) [10.58]
B''	1.386(2) [1.36]	1.192(2) [1.15]	1.390(4) [1.36]	1.548(6) [1.51]	1.335(3) [1.34]
C''	1.288(1) [1.27]	1.142(2) [1.11]	1.274(3) [1.27]	1.509(5) [1.46]	1.279(4) [1.27]
$\tilde{\epsilon}_{aa}$	-0.46(2) [-0.46]	-5.21(5) [-4.85]	-2.331(7) [-2.18]	-0.34(1) [-0.42]	-3.72(3) [-3.47]
$\tilde{\epsilon}_{bb}$	-0.30(1) [-0.33]	-0.09(2) [-0.06]	-0.14(2) [-0.15]	-0.261(9) [-0.23]	-0.03(1) [-0.00]
$\tilde{\epsilon}_{cc}$	-0.14(1) [-0.08]	0.00 [0.00]	-0.01(1) [-0.02]	-0.271(9) [-0.22]	0.03(1) [-0.03]
$ \tilde{\epsilon}_{ab} = \tilde{\epsilon}_{ba} $	0.22(4) [0.58]	0.52(1) [1.10]	0.44(2) [0.87]	0.41(3) [0.42]	-[0.14]
$ \tilde{\epsilon}_{bc} = \tilde{\epsilon}_{cb} $	0.19(4) [0.16]	0.00 [0.00]	-[0.05]	0.22(2) [0.22]	-[0.01]
$ \tilde{\epsilon}_{ac} = \tilde{\epsilon}_{ca} $	0.11(3) [0.30]	0.00 [0.05]	0.20(4) [0.30]	0.23(2) [0.22]	-[0.47]
A'	8.730(2) [9.14]	15.316(8) [15.81]	8.852(4) [9.13]	7.427(7) [7.60]	10.96(7) [11.15]
B'	1.414(1) [1.39]	1.173(2) [1.16]	1.392(1) [1.38]	1.577(3) [1.53]	1.308(3) [1.32]
C'	1.305(1) [1.29]	1.149(1) [1.12]	1.289(1) [1.28]	1.524(1) [1.49]	1.269(1) [1.26]
T ₀₀ (cm ⁻¹)	28643.38(1)	29012.82(1)	28986.98(1)	28640.35(1)	29121.57(1)
relative energies ^b	... [0.0]	... [19]	... [397]	... [390]	... [449]

^a The ground state constants correspond to an average of the values from all observed bands of a given conformer, weighted inversely by the standard deviation of the fit, σ . The excited-state constants correspond to the vibrationless level obtained from the fits of the origin bands A, C, B, a, and E, respectively. The rotational constants corresponding to the vibrationally excited states for conformers G₁T₂T₃, T₁T₂T₃, T₁T₂G₃, and T₁G₂T₃ obtained from bands G^a, F^b and J^c, I^d, and H^e, respectively, are A' = 8.796(7), B' = 1.429(2), C' = 1.308(1), T_{0G} = T₀₀+584.28(1); A' = 15.82(1), B' = 1.177(5), C' = 1.160(2), T_{0F} = T₀₀+127.98(1); A' = 15.521(4), B' = 1.175(1), C' = 1.160(1), T_{0J} = T₀₀+670.65(1); A' = 8.978(4), B' = 1.415(2), C' = 1.297(2), T_{0I} = T₀₀+666.43(1); and A' = 11.167(5), B' = 1.266(2), C' = 1.285(1), T_{0H} = T₀₀+110.64(1). The error quoted for the constants is one standard deviation. The calculated constants of the assigned conformers (of which the calculated values most closely match the experimental ones) are given in brackets. Ellipsis points indicate that corresponding experimental data is not available. ^b Relative energies (cm⁻¹) are for the \tilde{X} state.

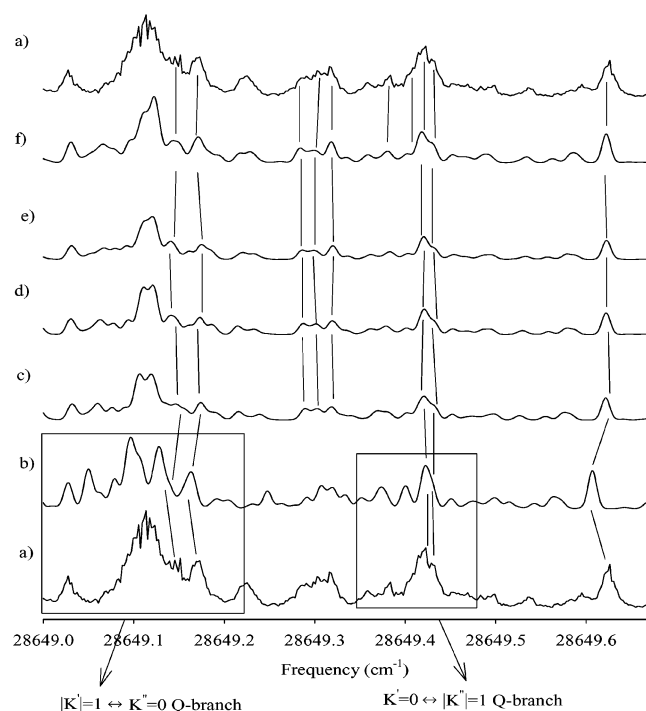


Figure 12. Spin-rotation coupling in the origin band of 1-butoxy: (a) expanded view of experimental spectrum of band A showing two Q-branches (in boxes); (b) simulation using refined (fit) rotational constants as demonstrated in Figure 11; (c) simulation obtained after fitting all three linear combinations of the rotational constants in the ground state; (d) simulation after fitting all six linear combinations of rotational constants in the ground and excited states; (e) simulation after fitting the spin-rotation constants ($a_0 + a/2$), ($a_0 - a$), and b ; (f) simulation after fitting six linear combinations of the rotational constants and five spin-rotation constants (see text for details).

pentyl ($\text{CH}_3\text{-}\dot{\text{C}}\text{H-(CH}_2\text{)}_2\text{-CH}_2\text{OH}$) radical has a cyclic structure, so it might be argued that the absence of these conformers is due to efficient relaxation to a conformation closely resembling the transition state, which retains sufficient energy from the photolysis to continue the tautomerization reaction.

TABLE 3: Vibrational Assignments of the Bands of 1-Butoxy and 1-Pentoxy^a

1-butoxy			1-pentoxy		
band	conformer	vibrational interval assignment	band	conformer	vibrational interval assignment
A	G ₁ T ₂	0 ₀ ⁰	A	G ₁ T ₂ T ₃	0 ₀ ⁰
B	T ₁ T ₂	0 ₀ ⁰	G	G ₁ T ₂ T ₃	634 ν_{CO}
D	T ₁ T ₂	169 ν_{CCO}	C	T ₁ T ₂ T ₃	0 ₀ ⁰
F	T ₁ T ₂	671 ν_{CO}	F	T ₁ T ₂ T ₃	128 ν_{CCO}
C	T ₁ G ₂	0 ₀ ⁰	J	T ₁ T ₂ T ₃	671 ν_{CO}
E	T ₁ G ₂	200 ν_{CCO}	K	T ₁ T ₂ T ₃	799 $\nu_{\text{CO}} + \nu_{\text{CCO}}$
			B	T ₁ T ₂ G ₃	0 ₀ ⁰
			I	T ₁ T ₂ G ₃	666 ν_{CO}
			a	G ₁ T ₂ G ₃	0 ₀ ⁰
			E	T ₁ G ₂ T ₃	0 ₀ ⁰
			H	T ₁ G ₂ T ₃	111 ν_{CCO}

^a ν_{CO} is the C–O stretch, and ν_{CCO} is the backbone C–C–O deformation.

Further experiments are certainly necessary to confirm or disprove this hypothesis. Indeed “more” cyclic conformers might be present but just have low quantum yields for fluorescence even from the vibrationless level. However, it is interesting to note that the postulated existence and accessibility of a tautomerization sink for the alkoxy radicals also would largely rationalize some previously reported, somewhat contradictory results. Dibble and co-workers^{14,15} carried out flow experiments with $T > 200$ K on 14 structural isomers of butoxy, pentoxy, and hexoxy. They reported observing assignable, structured spectra for only 4 of the 14 isomers, namely, 2-butoxy, *t*-butoxy, *t*-pentoxy, and 3-pentoxy. On the other hand, we have observed strong LIF spectra for all 13 structural isomers that we have investigated under jet-cooled conditions ($T < 1.5$ K). (The isomer neopentoxy was not observed because, as revealed by FTIR absorption spectra, we were unable to synthesize the precursor by the standard procedures referenced in the Experimental Section.) The key observation is that, of the 14 possible structural isomers of butoxy, pentoxy, and hexoxy, only the four for which Dibble and co-workers observed LIF spectra do not have cyclic conformers and cannot form a six-member ring

transition state. We would expect that conformer conversion would remain facile on the temperature and time scale of the experiments of Dibble and co-workers. Therefore, a tautomerization sink might well have destroyed the population of the 10 isomers of which the LIF spectra could not be observed in those experiments.

On the other hand, in our jet experiment, it is clear that conformers get “frozen out” far from equilibrium. Our detailed rotational analyses demonstrate that most, if not all, of our observed LIF spectra are assignable to conformers of which the geometries are quite different from the cyclic transition state required for tautomerization. This may well be the explanation of why we have observed strong LIF spectra from all of these structural isomers, when previous experiments did not.

8. Conclusions

We have recently reported that the jet-cooled LIF spectrum of 1-propoxy consists of two independent spectra belonging to the T and G conformers. In this work, we have extended our analysis of the $\tilde{B}-\tilde{X}$ transition in the alkoxy radicals to 1-butoxy and 1-pentoxy and obtained rotational and spin-rotation constants for them.

Using the method of rotational bar coding, we can unambiguously assign six separate bands of 1-butoxy to three distinct conformers, namely, the T_1T_2 , G_1T_2 , and T_1G_2 forms. All analyzed lines terminate on either the electronic origin or excited vibrational levels of the \tilde{B} state of these conformers. Similarly, we assign 11 bands of the $\tilde{B}-\tilde{X}$ spectrum of 1-pentoxy to conformers identified as the $T_1T_2T_3$, $T_1T_2G_3$, $T_1G_2T_3$, $G_1T_2T_3$, and $G_1T_2G_3$ forms.

By a combination of experimental electronic origins and computational results, we can learn a considerable amount about subtle stabilization effects depending on molecular geometry. Such effects allow us to “understand” the T_{00} values of the $\tilde{B}-\tilde{X}$ transition for different groups of conformers and may have implications for molecules as large as proteins.

Besides the direct structural information that we obtain from the spectra, our isomer- and conformer-specific diagnostic allows us to conclude some interesting facts about the radicals’ dynamics. As with 1-propoxy, all conformers of both 1-butoxy and 1-pentoxy show limited vibrational structure before a nonradiative decay channel opens to quench the fluorescence (and the LIF spectra).

It is clear that the sample of conformers that we observe is far from equilibrium. Rather, a number of higher-energy (with respect to the kT in the jet) conformers appear to be frozen out, but some comparably energetic conformers are “missing”. We postulate that a possible sink for these conformers is the tautomerization reaction to form hydroxy alkyl radicals. Conformer geometries comparable to the cyclic transition state of this reaction are most likely to be consumed.

Acknowledgment. The authors acknowledge the help of Chris Carter in taking some of the initial data on the butoxy and pentoxy spectra. We gratefully acknowledge the support of parts of this work by the National Science Foundation via Grant CHE-0211281. Other parts of this work were supported by the Chemical Sciences, Geosciences and Biosciences Divi-

sion, Office of Basic Energy Sciences, Office of Science, U.S. Department of Energy, via Grant DE-FG02-01ER15172.

Supporting Information Available: A detailed description of the analysis of the rotational structure of the 1-pentoxy radical including experimental and simulated spectra. This material is available free of charge via the Internet at <http://pubs.acs.org>.

References and Notes

- (1) Foster, S. C.; Misra, P.; Lin, T.-Y.; Damo, C. P.; Carter, C. C.; Miller, T. A. *J. Phys. Chem.* **1988**, *92*, 5914.
- (2) Liu, X.; Damo, C. P.; Lin, T.-Y.; Foster, S. C.; Misra, P.; Yu, L.; Miller, T. A. *J. Phys. Chem.* **1989**, *93*, 2266.
- (3) Powers, D. E.; Pushkarsky, M.; Miller, T. A. *J. Chem. Phys.* **1997**, *106*, 6863.
- (4) Inoue, G.; Akimoto, H.; Okuda, M. *Chem. Phys. Lett.* **1979**, *63*, 213.
- (5) Ohbayashi, K.; Akimoto, H.; Tanaka, I. *J. Phys. Chem.* **1977**, *81*, 798.
- (6) Wendt, H. R.; Hunziker, H. E. *J. Chem. Phys.* **1979**, *71*, 5202.
- (7) Style, D. W. G.; Ward, J. C. *Trans. Faraday Soc.* **1953**, *49*, 999.
- (8) Ebata, T.; Yanagishita, H.; Obi, K.; Tanaka, I. *Chem. Phys.* **1982**, *69*, 27.
- (9) Inoue, G.; Okuda, M.; Akimoto, H. *J. Chem. Phys.* **1981**, *75*, 2060.
- (10) Tan, X. Q.; Williamson, J. M.; Foster, S. C.; Miller, T. A. *J. Phys. Chem.* **1993**, *97*, 9311.
- (11) Bai, J.; Okabe, H.; Halpern, J. B. *Chem. Phys. Lett.* **1988**, *149*, 37.
- (12) Ohbayashi, K.; Akimoto, H.; Tanaka, I. *J. Phys. Chem.* **1977**, *81*, 798.
- (13) Carter, C. C.; Atwell, J.; Gopalakrishnan, S.; Miller, T. A. *J. Phys. Chem. A* **2000**, *104*, 9165.
- (14) Wang, C.; Shemesh, L. G.; Deng, W.; Lilien, M. D.; Dibble, T. S. *J. Phys. Chem. A* **1999**, *103*, 8207–8212.
- (15) Wang, C.; Deng, W.; Shemesh, L.; Lilien, M. D.; Katz, D. R.; Dibble, T. S. *J. Phys. Chem. A* **2000**, *104*, 10368.
- (16) Tserapi, A. D.; Miller, T. A. *J. Appl. Phys.* **1994**, *75*, 7231.
- (17) Gopalakrishnan, S.; Carter, C. C.; Zu, L.; Stakhursky, V.; Tarczay, G.; Miller, T. A. *J. Chem. Phys.* **2003**, *118*, 4954.
- (18) Blatt, A. H. *Organic Synthesis, Collective Volume*; Wiley: New York, 1943.
- (19) Liu, X.; Foster, S. C.; Williamson, J. M.; Yu, L.; Miller, T. A. *Mol. Phys.* **1990**, *69*, 357.
- (20) Foster, S. C.; Miller, T. A. The Spectroscopy of Transient Species in Supersonic Free Jet Expansions. In *Applications of Lasers in Chemistry*; Evans, D. K., Ed.; Marcel Dekker: New York, 1989; p 307.
- (21) Foster, S. C.; Kennedy, R. A.; Miller, T. A. Laser Spectroscopy of Chemical Intermediates in Supersonic Free Jet Expansions. In *Frontiers of Laser Spectroscopy of Gases*; Alves, A. C. P., Brown, J. M., Hollas, J. M., Eds.; Nato ASI Series; Kluwer Academic Publishers: Dordrecht, The Netherlands, 1988; p 421.
- (22) Zare, R. N. *Angular Momentum*; Wiley-Interscience: New York, 1988.
- (23) Brown, J. M.; Sears, T. J. *J. Mol. Spectrosc.* **1979**, *75*, 111.
- (24) Brown, J. M.; Sears, T. J.; Watson, J. K. G. *Mol. Phys.* **1980**, *41*, 173.
- (25) Raynes, W. T. *J. Chem. Phys.* **1961**, *41*, 3020–3032.
- (26) Tarczay, G.; Gopalakrishnan, S.; Miller, T. A. *J. Mol. Spectrosc.*, in press.
- (27) Frisch, M. J.; Trucks, G. W.; Schlegel, H. B.; Scuseria, G. E.; Robb, M. A.; Cheeseman, J. R.; Zakrzewski, V. G.; Montgomery, J. A., Jr.; Stratmann, R. E.; Burant, J. C.; Dapprich, S.; Millam, J. M.; Daniels, A. D.; Kudin, K. N.; Strain, M. C.; Farkas, O.; Tomasi, J.; Barone, V.; Cossi, M.; Cammi, R.; Mennucci, B.; Pomelli, C.; Adamo, C.; Clifford, S.; Ochterski, J.; Petersson, G. A.; Ayala, P. Y.; Cui, Q.; Morokuma, K.; Malick, D. K.; Rabuck, A. D.; Raghavachari, K.; Foresman, J. B.; Cioslowski, J.; Ortiz, J. V.; Stefanov, B. B.; Liu, G.; Liashenko, A.; Piskorz, P.; Komaromi, I.; Gomperts, R.; Martin, R. L.; Fox, D. J.; Keith, T.; Al-Laham, M. A.; Peng, C. Y.; Nanayakkara, A.; Gonzalez, C.; Challacombe, M.; Gill, P. M. W.; Johnson, B. G.; Chen, W.; Wong, M. W.; Andres, J. L.; Head-Gordon, M.; Replogle, E. S.; Pople, J. A. *Gaussian 98*, revision A.7; Gaussian, Inc.: Pittsburgh, PA, 1998.